JACS
JOURNAL OF THE AMERICAN CHEMICAL SOCIETY
pubs.acs.org/JACS
Article

Visible-Light Photocatalyzed *peri*-(3 + 2) Cycloadditions of Quinolines

Peter Bellotti,[⊥] Torben Rogge,[⊥] Fritz Paulus,[⊥] Ranjini Laskar, Nils Rendel, Jiajia Ma, K. N. Houk,* and Frank Glorius*

Cite This: *J. Am. Chem. Soc.* 2022, 144, 15662−15671
Read Online
ACCESS | Metrics & More | Article Recommendations | Supporting Information

ABSTRACT: Cycloaddition reactions—epitomized by the Diels−Alder reaction—offer an arguably unmatched springboard for achieving chemical complexity, often with excellent selectivity, in a modular single step. We report the synthesis of aza-acenaphthenes in a single step by an unprecedented formal *peri*-(3 + 2) cycloaddition of simple quinolines with alkynes. A commercially available iridium complex exerts a dual role of photosensitizer and photoredox catalyst, fostering a cyclization/rearomatization cascade. The initial energy-transfer phase leads to the acenaphthene skeleton, while the ensuing redox shuttling step leads to aromatization. We applied this technology to 8-substituted quinolines and phenanthrolines, which smoothly reacted with both terminal and internal alkynes with excellent levels of regio- and diastereoselectivity. Density functional theory calculations revealed the intertwined EnT/SET nature of the process and offered guiding design principles for the synthesis of new aza-acenaphthenes.

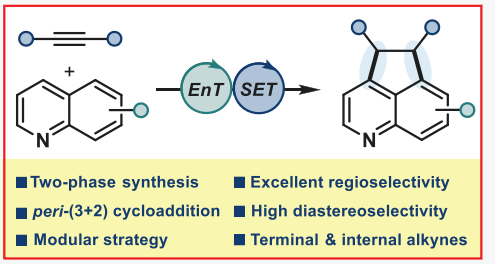

INTRODUCTION

The power of cycloaddition reactions does not exclusively emanate from the well-choreographed growth of molecular complexity but climaxes in the generation of valuable molecular frameworks. Venerable cycloadditions such as the Diels−Alder reaction have stimulated the disconnection approach toward natural product synthesis.[1] Aza-acenaphthenes represent an architecture found in both natural products (e.g., delavatine A)[2] and drug candidates (e.g., camptothecin analogue,[3] HIV integrase inhibitors[4]) (Figure 1A). In contrast to acenaphthene, which can be obtained from coal tar (approximately 0.3%),[5] aza-acenaphthenes require step-intensive syntheses, thus hampering their widespread utilization in medicinal chemistry endeavors. In the formal synthesis of (+)-delavatine A, Koert and co-workers leveraged a visible-light-induced intramolecular ring closure to forge the ethano bridge from pendant olefins.[2b,6a−e] Shen, Li, and Zhang[2a]—as well as Liu and Sarpong[2c,d]—opted for the de novo formation of the heteroaromatic fragment via intramolecular ring closure or condensation from highly decorated precursors, respectively.[3,4,7,8]

Recently, energy-transfer photocatalysis (EnT)[9a−c] emerged as a pluripotent-enabling tool toward dearomative cycloadditions, which are both thermodynamically and kinetically restrained (Figure 1B).[10] Harnessing the energy of visible-light photons often leads to compressed kinetic barriers—surmountable at room temperature—and prevents undesired cycloreversion due to highly energetic irradiation. Zheng, Zhang, and You,[11a−c] Oderinde,[11d,e] König,[11f] Glorius,[11g,h] and others[11i] developed (2 + 2) dearomative cycloadditions of electron-rich benzo-condensed (hetero)aromatics, both intra- and intermolecularly. Topological upgrading via remote position bridging—in a formal (4 + 2) reaction mode—was pioneered by Brown, Houk, and Glorius[12a,b] in the context of electron-poor aza-arene dearomative cycloaddition.[12c,d]

We envisaged that energy transfer might enable the de novo synthesis of aza-acenaphthenes from simple aza-arenes in a *peri*-(3 + 2) cycloaddition fashion. This strategy potentially obviates the need for prefunctionalized precursors—and thus tedious syntheses[2−4,7,8]—and concomitantly fosters user-friendly modular substitution exploration at the ethano bridge and the heterocyclic core. Notwithstanding, EnT-based *peri*-cycloadditions face proscriptive challenges: (a) diversion of the usual monocyclic reactivity toward positions located on different rings, (b) reaction reversibility, and (c) requirement for rearomatization.[13] Cognizant that the synthesis of complex products can be achieved leveraging domino processes,[14] we envisioned that visible-light photocatalysis could foster both the cyclization and the rearomatization phase to generate aza-acenaphthenes (Figure 1C). Specifically, energy transfer can potentially empower the cyclization stage, while the ensuing phase would leverage the electron-shuttle ability of the photocatalyst. Thus far, the multiple EnT/SET photocatalytic

Received: June 1, 2022
Published: August 19, 2022

https://doi.org/10.1021/jacs.2c05687
J. Am. Chem. Soc. 2022, 144, 15662−15671

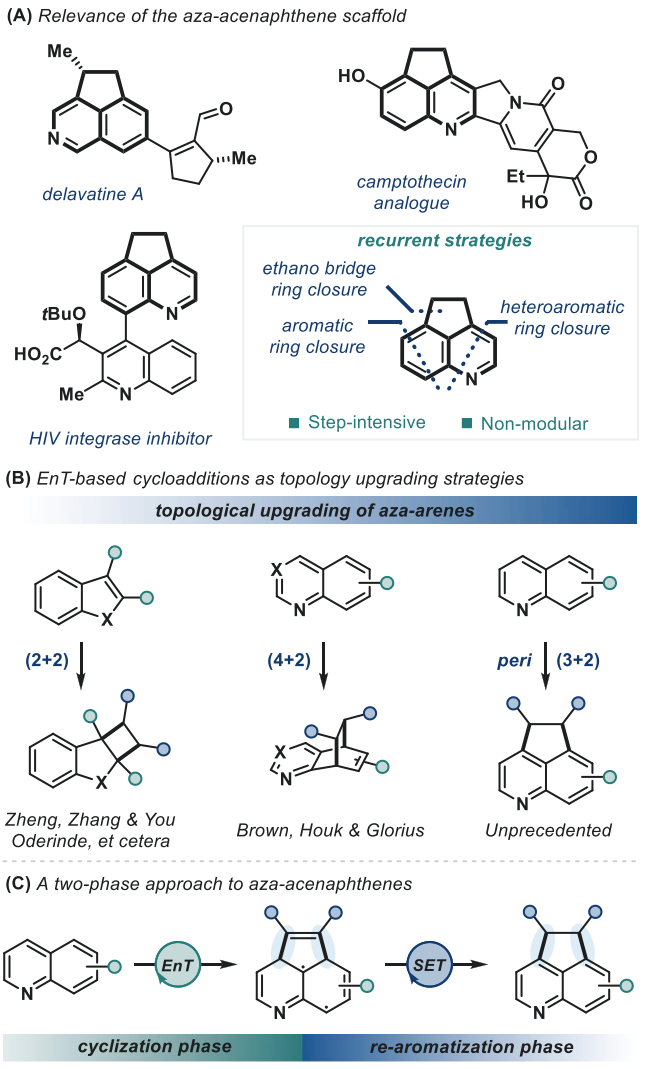

Figure 1. (A) Aza-acenaphthene scaffolds in natural products and medicinal chemistry-relevant compounds. Common synthetic disconnections. (B) Energy-transfer-based cycloaddition reactions toward topological upgrading. (C) Our strategy: two-phase approach toward *peri*-bridged aza-acenaphthenes.

activation mode—independently pioneered by Lu and Xiao[15a] and Gilmour and co-workers[15b]—has remained largely circumscribed to dinitrogen extrusion[15a,c−f] and $E \rightarrow Z$ isomerization.[15b,g,h]

While dearomative thermal (3 + 2) cycloaddition reactions—utilizing in particular nitrosubstituted aromatics—have reached remarkable levels of sophistication,[16] the corresponding energy-transfer-based reactions have remained elusive. In this report, we present the successful implementation of a "two-phase" approach based on a single photocatalytic species capable of generating aza-acenaphthenes from simple quinolines and alkynes. Leveraging two distinct activation modes—namely, triplet energy- and single-electron transfer—a *peri*-(3 + 2) cycloaddition (cyclization phase) was efficiently coupled with a rearomatization phase.

RESULTS AND DISCUSSION

Reaction Development. Quinolines can undergo efficient energy-transfer quenching of photoexcited [Ir(dF(CF$_3$)ppy)$_2$(dtbbpy)][PF$_6$] ([**Ir-F**][**PF$_6$**], E_T = 61.8 kcal mol^{-1}).[12b] Initial attempts to achieving the desired (3 + 2) cycloaddition with unsubstituted quinoline, 3-trifluoromethylquinoline and dimethyl 1,8-naphthalene carboxylate were unsuccessful, with no detectable *peri*-bridged product (Table 1, upper). We postulated that tuning the redox properties by installing electron-withdrawing groups (EWGs) at different ring positions could divert the initial alkyne addition to the desired rearomative phase. In fact, initial density functional theory (DFT) calculations suggested that EWG groups could render the turnover of Ir(II) to Ir(III) in the rearomatization phase thermodynamically more feasible. Attempts with methyl 6-

Table 1. Initial Feasibility Screening, Selected Optimization, and Condition-Based Sensitivity Screening[a,b,c,d,e]

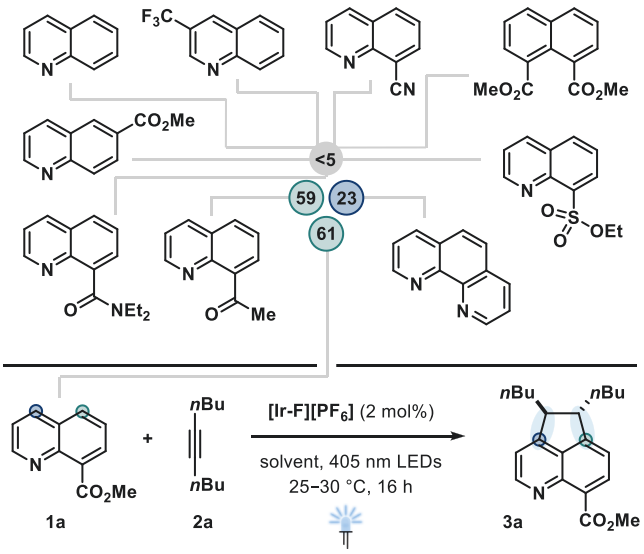

Entry[b]	Conditions	Yield %[c]	Entry[b]	Conditions	Yield %[c]
1	HFIP as solvent	61	6[d]	1.0 equiv of **2a**	49
2	TFE as solvent	<5	7[d]	10.0 equiv of **2a**	51
3	MeOH as solvent	<5	8[d]	450 nm LEDs	36
4	CH_2Cl_2 as solvent	<5	9[d]	in darkness	<5
5[d,e]	2.0 equiv of HCl	<5	10[d]	without **[Ir-F][PF$_6$]**	<5

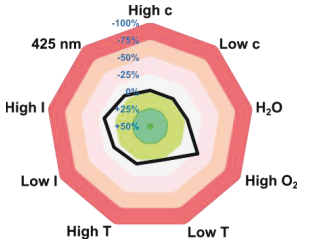

Condition-based sensitivity screening

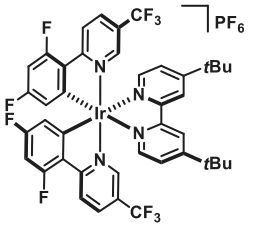

[Ir(dF(CF$_3$)ppy)$_2$(dtbbpy)][PF$_6$]
[Ir-F][PF$_6$]

[a]Screening conditions: aza-arene (0.1 mmol, 1.0 equiv), **2a** (0.5 mmol, 5.0 equiv), [Ir(dF(CF$_3$)ppy)$_2$(dtbbpy)][PF$_6$] (2 μmol, 2 mol %), HFIP (500 μL, 0.2 M), 18 W 405 nm LEDs, 25−30 °C, 16 h. Yields are reported in %. [b]Standard reaction conditions: **1a** (0.1 mmol, 1.0 equiv), **2a** (0.5 mmol, 5.0 equiv), [**Ir-F**][**PF$_6$**] (2 μmol, 2 mol %), solvent (500 μL, 0.2 M), 18 W 405 nm LEDs, 25−30 °C, 16 h. [c]Yields were obtained using ^{1}H NMR spectroscopy with mesitylene as the internal standard. [d]Using HFIP (500 μL, 0.2 M) as the solvent. [e]HCl 4 M in 1,4-dioxane was used. For experimental details, see the Supporting Information.

https://doi.org/10.1021/jacs.2c05687
J. Am. Chem. Soc. 2022, 144, 15662−15671

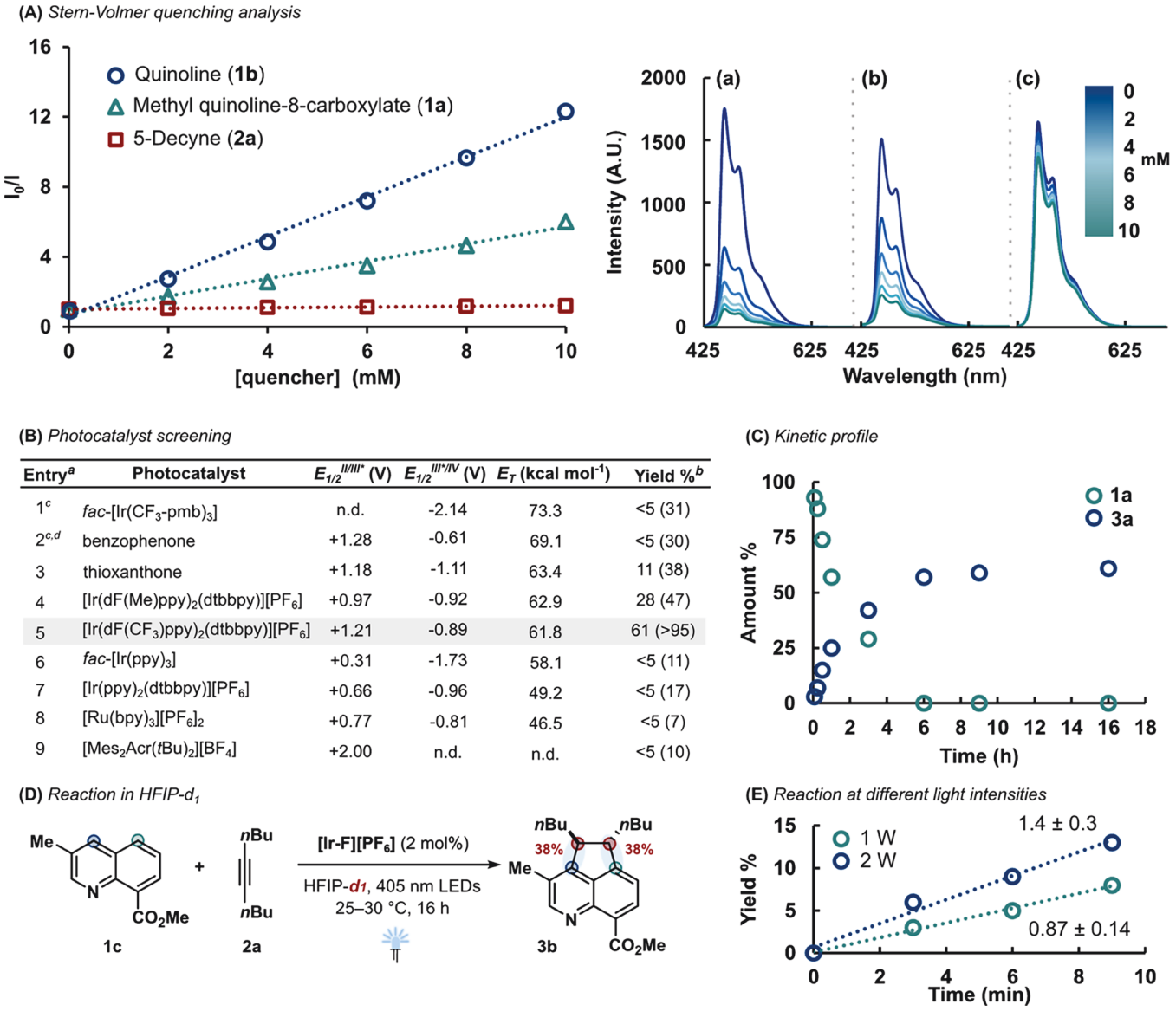

Entry[a]	Photocatalyst	$E_{1/2}^{II/III*}$ (V)	$E_{1/2}^{III*/IV}$ (V)	E_T (kcal mol^{-1})	Yield %[b]
1[c]	*fac*-[Ir(CF$_3$-pmb)$_3$]	n.d.	-2.14	73.3	<5 (31)
2[c,d]	benzophenone	+1.28	-0.61	69.1	<5 (30)
3	thioxanthone	+1.18	-1.11	63.4	11 (38)
4	[Ir(dF(Me)ppy)$_2$(dtbbpy)][PF$_6$]	+0.97	-0.92	62.9	28 (47)
5	[Ir(dF(CF$_3$)ppy)$_2$(dtbbpy)][PF$_6$]	+1.21	-0.89	61.8	61 (>95)
6	*fac*-[Ir(ppy)$_3$]	+0.31	-1.73	58.1	<5 (11)
7	[Ir(ppy)$_2$(dtbbpy)][PF$_6$]	+0.66	-0.96	49.2	<5 (17)
8	[Ru(bpy)$_3$][PF$_6$]$_2$	+0.77	-0.81	46.5	<5 (7)
9	[Mes$_2$Acr(*t*Bu)$_2$][BF$_4$]	+2.00	n.d.	n.d.	<5 (10)

Figure 2. Selected mechanistic experiments. (A) Stern−Volmer quenching analysis for quinoline (**1b**) (a), methyl quinoline-8-carboxylate **1a** (b), and 5-decyne **2a** (c). (B) Photocatalyst screening. [a]Reaction conditions: **1a** (0.1 mmol, 1.0 equiv), **2a** (0.5 mmol, 5.0 equiv), photocatalyst (2 μmol, 2 mol %), HFIP (500 μL, 0.2 M), 18 W 405 nm LEDs, 25−30 °C, 16 h. [b]Yields and conversions (in parentheses) were obtained using ^{1}H NMR spectroscopy with mesitylene as the internal standard. [c]365 nm LEDs were used. [d]20 mol % benzophenone was used. $E_{1/2}$ (given vs SCE) and E_T values were obtained from refs 18. (**C**) Kinetic profile of the reaction. Performed according to Table 1, entry 1, using quinoline **1a** (0.1 mmol) and alkyne **2a** (5.0 equiv). (D) Reaction in HFIP-d_1. (E) Reaction initial rate kinetic profile at different light intensities [1 W (green) and 2 W (blue)]. Performed according to Table 1, entry 1, using quinoline **1a** (0.1 mmol) and alkyne **2a** (5.0 equiv). Slope uncertainties are reported at 2σ (~95.4% in normal distribution). For experimental details, see the Supporting Information. bpy = 2,2′-Bipyridine, dF(CF$_3$)ppy = 2-(2,4-difluorophenyl)-5-trifluoromethylpyridine-*N*,C$_{20}$, dF(Me)ppy = 2-(2,4-difluorophenyl)-5-methylpyridine-*N*,C$_{20}$, dtbbpy = 4,4′-di-*tert*-butyl-2,2′-dipyridyl, Mes$_2$Acr-(*t*Bu)$_2$ = 3,6-di-*tert*-butyl-9,10-dimesitylacridinium, n.d. = value not defined in the literature, and ppy = 2-(2-pyridinyl)phenyl-C,*N*.

quinoline carboxylate, 8-cyanoquinoline, ethyl quinoline-8-sulfonate, and *N*,*N*-diethylquinoline-8-carboxamide proved unfruitful. Conversely, methyl(quinolin-8-yl)methanone and phenanthroline showed promising reactivity (59% and 23% yields, respectively). Replacing the ketone group for 8-substituted ester **1a**, with 5-decyne **2a** in hexafluoro-2-propanol (HFIP, pK_a = 9.3)[17a−c] and 405 nm light irradiation delivered *peri*-bridged product **3a** in a 61% yield and with excellent *anti*-diastereoselectivity (>95:5 d.r.).

Compared to the reaction of **1a** with enol esters, which proceeds in (2 + 2) cycloaddition fashion,[12d] alkyne **2a** affords exquisite *peri*-(3 + 2) selectivity. 2,2,2-Trifluoroethanol (TFE, pK_a = 12.4),[17d] methanol, or dichloromethane as the solvent proved unsuitable (entries 2−4), but to our surprise, the addition of Brønsted acid completely suppressed product **3a** formation (entry 5). Reducing or increasing the excess of alkyne partner caused the yield to decrease slightly to 49 and 51%, respectively (entries 6 and 7). Irradiation at 450 nm was less effective (36%, entry 8), and conduction of the process in darkness or without [**Ir-F**][**PF$_6$**] photocatalyst confirmed that both visible-light and photocatalyst are required (entries 9 and 10). Condition-based sensitivity screening[19] revealed the detrimental effect of molecular oxygen and high light intensity. In the former case, O_2 can act as a triplet quencher, while the

https://doi.org/10.1021/jacs.2c05687
J. Am. Chem. Soc. 2022, 144, 15662−15671

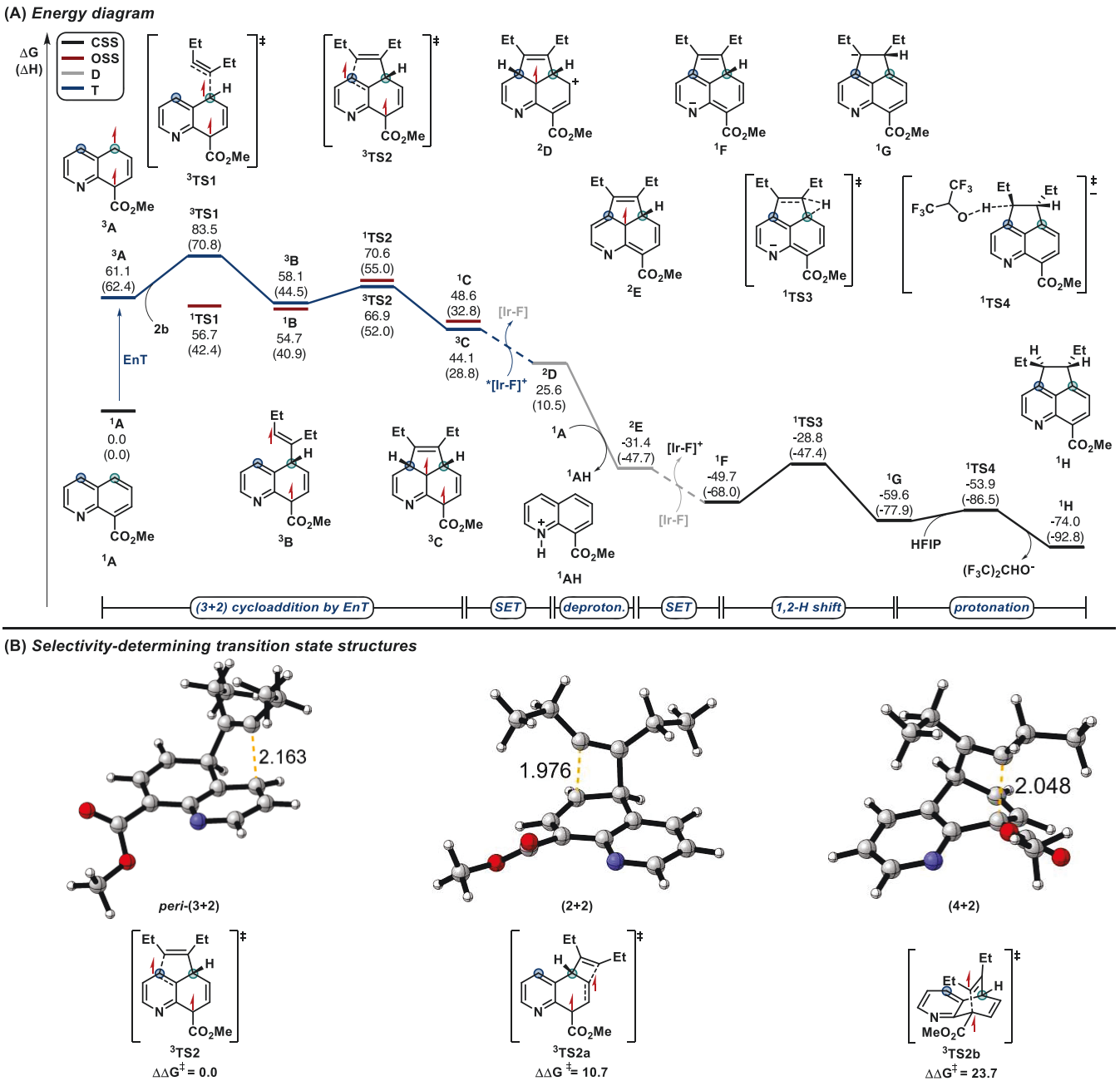

Figure 3. (A) Calculated energy diagram (in kcal mol^{-1}) for the reaction of quinoline **1a** with 3-hexyne (**2b**). Superscripts correspond to the spin state. CSS = closed-shell singlet, OSS = open-shell singlet, D = doublet, T = triplet. (B) Calculated transition state structures and relative Gibbs free energies (in kcal mol^{-1}) for *peri*-(3 + 2) cycloaddition, (2 + 2) cycloaddition, and (4 + 2) cycloaddition. Distances are given in angstrom (Å). For computational details, see the Supporting Information.

latter instance can be tentatively ascribed to the photopromoted product decomposition. Modest variations in concentration, wet solvent, reduced or increased temperature, reduced light intensity, and irradiation with a 425 nm light source were largely inconsequential to the reaction yield, thus testifying to the robustness of the reaction protocol.

Mechanistic Investigation. To shed light upon our dual EnT/SET mechanistic hypothesis, we conducted thorough mechanistic experiments. The Stern−Volmer luminescence quenching analysis using quinoline (**1b**), quinolyl ester **1a**, and 5-decyne **2a** showed that both heteroaromatic species—albeit with different efficiency—can quench [**Ir-F**][$\mathbf{PF_6}$]. On the other hand, 5-decyne (**2a**) did not significantly attenuate [**Ir-F**][$\mathbf{PF_6}$] fluorescence (Figure 2a). Considering that quinoline (**1b**) does not productively react in the reaction suggests that the efficient photocatalyst quenching is not the sole parameter that determines the desired reactivity. We then examined different organic- and metal-based photocatalysts, covering a wide E_T and redox window (Figure 2b). A distinctly nonmonotonous relationship between yield and triplet energy, showing a "sweet spot" at 62−63 kcal mol^{-1} (entries 4 and 5), was observed. This observation questions the operativity of a purely EnT-based pathway.[20] Sensitizers with increasingly high triplet energies—thioxanthone (entry 3), benzophenone (entry 2), and *fac*-[Ir(CF-pmb)$_3$] (entry 1)—failed at providing substantial amounts of **3a**, thus suggesting that

https://doi.org/10.1021/jacs.2c05687
J. Am. Chem. Soc. 2022, 144, 15662−15671

Table 2. Substrate Scope with (A) Disubstituted Alkynes, (B) Monosubstituted Alkynes, and (C) Aza-arenes[a,b,c,d,e,f]

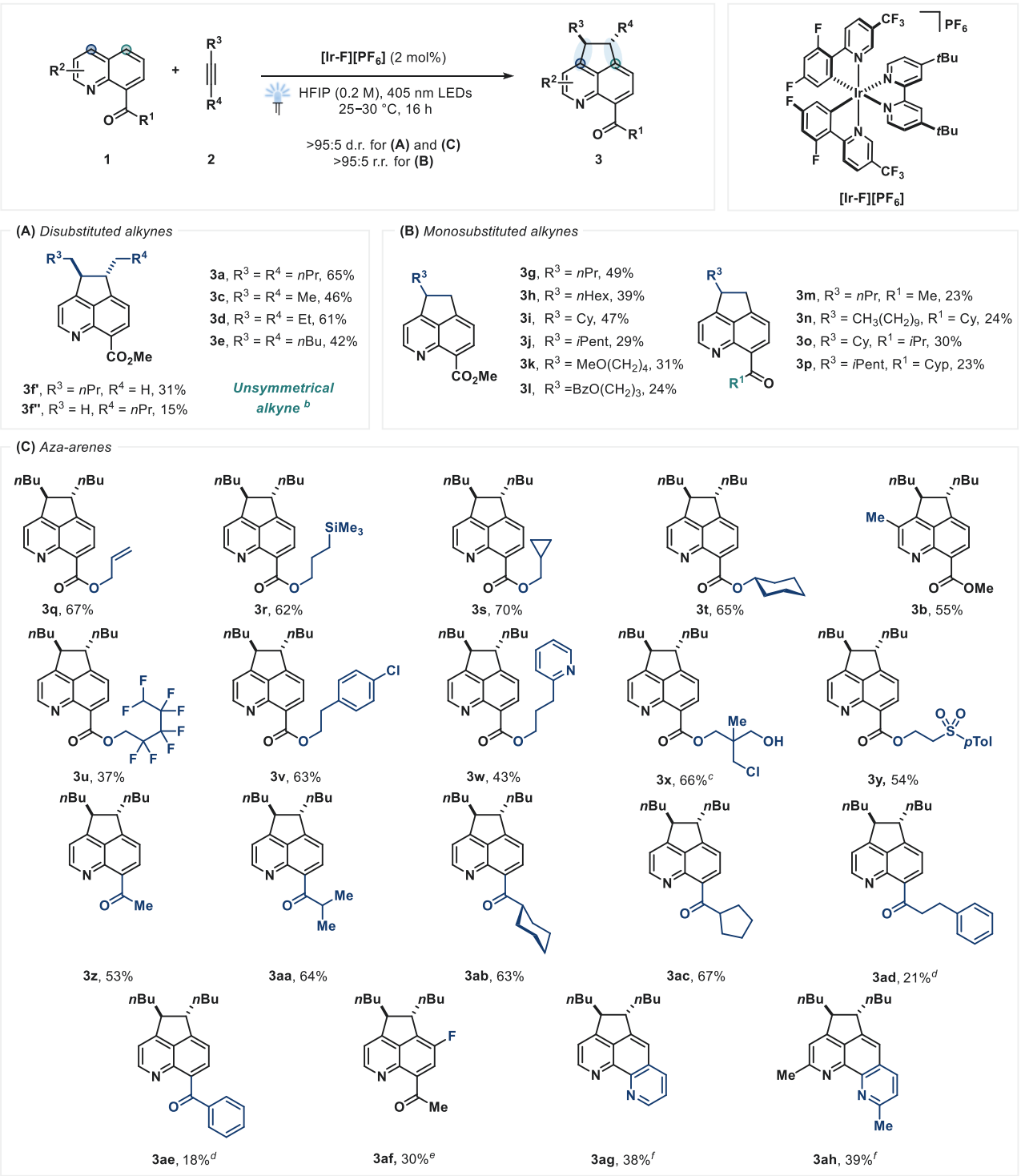

[a]Isolated yields are reported, regio- and diastereoselectivities were higher than 95:5. Standard reaction conditions: **1** (0.2 mmol, 1.0 equiv), **2** (1.0 mmol, 5.0 equiv), [**Ir-F**][PF_6] (4 μmol, 2 mol %), HFIP (0.2 M), 18 W 405 nm LEDs, 25−30 °C, 16 h. [b]r.r. Value of the crude reaction mixture is approximately 1:1. [c]Reaction was performed at 0.175 mmol scale. The d.r. ratio refers to the *peri*-substituents. No diastereoinduction from the quaternary stereocenter could be observed. [d]10 equiv **2a**, 4 mol % [**Ir-F**][PF_6] were used, and the reaction time was increased to 60 h. [e]Ring-opening side product was observed. The crude yield was determined by ^{1}H NMR, using mesitylene as the internal standard. [f]10 equiv **2a**, 4 mol % [**Ir-F**][PF_6] were used, and the reaction time was increased to 48 h. For experimental details, see the Supporting Information. Cyp = cyclopentyl; *p*Tol = *para*-tolyl.

elevated E_T alone does not suffice as the criteria for efficient photocatalysis. Extremely reducing *fac*-[Ir(CF-pmb)$_3$] ($E_{1/2}^{PC*/PC+\bullet}$ = −2.14 V vs SCE, entry 1) and *fac*-[Ir(ppy)$_3$] ($E_{1/2}^{PC*/PC+\bullet}$ = −1.73 V vs SCE, entry 6) did not afford any product, thus speaking against a combination of EnT/oxidative quenching. Photocatalysts possessing E_T values below 60 kcal

https://doi.org/10.1021/jacs.2c05687
J. Am. Chem. Soc. 2022, 144, 15662−15671

mol^{-1} (entries 6−8) performed equally unsatisfactorily, even when a highly oxidizing acridinium-based photocatalyst was used ($E_{1/2}^{PC*/PC-\bullet}$ = +2.00 V vs SCE, entry 9). Kinetic profiling of the reaction between **1a** and **2a** revealed complete starting material consumption within 6 h, following a pseudo-first-order kinetic (Figure 2C). Cyclic voltammetry measurement of the reduction potential of **1a** ($E_{p/2}$ = −1.87 V vs SCE in MeCN) revealed that *[**Ir-F**][PF_6] cannot undergo oxidative quenching with the substrate (paragraph 8.5 in the Supporting Information).

To gain further insight into the mechanism of the diastereoselective (3 + 2) cycloaddition, we performed density functional theory (DFT) calculations on the reaction of quinoline **1a** with 3-hexyne (**2b**) at the ωB97X-D/def2-QZVPP + SMD (Eps = 16.7; EpsInf = 1.625625)//ωB97X-D/def2-TZVP + SMD (Eps = 16.7; EpsInf = 1.625625) level of theory (Figure 3A).[21] Initially, triplet quinoline ^{3}**A** is generated by energy transfer from the excited photosensitizer *[**Ir-F**]$^+$ to 8-ester-substituted quinoline ^{1}**A**. ^{3}**A** readily reacts with alkyne **2b**, likely via spin-crossover from the triplet to the lower-lying open-shell singlet transition state ^{1}**TS1** to yield intermediate ^{1}**B** or ^{3}**B**. Subsequent selective C−C bond formation at the quinoline 4-position via transition state **TS2** with an activation free energy of 12−13 kcal mol^{-1} on either triplet or singlet surfaces forms a diradical intermediate **C**. In comparison, the radical attack onto the 6- or 8-position required 10.7 and 23.7 kcal mol^{-1} higher activation free energies, respectively, which can be rationalized by a significantly increased ring strain in ^{3}**TS2a** and ^{3}**TS2b** due to the forming cyclobutene and bicyclo[2.2.2]octadiene motifs (Figure 3B and Supporting Figure 31 in the Supporting Information). **C** is likely to be oxidized by excited *[**Ir-F**]$^+$ within a reductive quenching cycle to yield radical cation ^{2}**D**. Thermodynamically favorable deprotonation with ^{1}**A** or HFIP anion (($F_3C)_2CHO^-$) at the 4-position generates intermediate ^{2}**E** (Supporting Figure 28 in the Supporting Information). Thereafter, ^{2}**E** is reduced by [**Ir-F**], thus regenerating the active photoredox catalyst [**Ir-F**]$^+$ and forming anionic intermediate ^{1}**F**, which subsequently undergoes 1,2-H shift via ^{1}**TS3** with an activation free energy of 20.9 kcal mol^{-1}. Finally, the facile protonation of ^{1}**G** with HFIP via ^{1}**TS4** with an activation free energy of only 5.7 kcal mol^{-1} delivers the observed, thermodynamically favorable *anti*-product ^{1}**H**. In contrast, the *syn*-configured product was found to be 2.7 kcal mol^{-1} less stable than the *anti*-diastereomer due to an increased destabilizing steric interaction between the two ethyl substituents (Supporting Figure 29 in the Supporting Information). Reaction performance in HFIP-d_1 showed significant deuterium incorporation (38%) at the *peri*-bridge, further supporting the solvent assistance in the proton shift process (Figure 2D). Furthermore, calculations on quinolines containing various electron-withdrawing as well as electron-donating substituents revealed the oxidation of the corresponding intermediate ^{3}**C** to be thermodynamically more favorable with electron-poor quinolines (Supporting Figure 32 in the Supporting Information). In contrast, electron-rich quinolines resulted in a significantly less facile reduction of intermediate ^{2}**E** (Supporting Figure 33 in the Supporting Information). An alternative mechanism involving energy transfer to ^{1}**A** immediately followed by single-electron transfer from a second molecule of excited photosensitizer to ^{3}**A** is unlikely to be operative due to an unfeasibly high activation free energy (Supporting Figure 34 in the Supporting Information).[22] In addition, we observed a linear initial rate growth—within experimental uncertainty—upon increasing light intensity (Figure 2E). This observation for the regioselective (3 + 2) cycloaddition diverges from the quadratic relationship reported by König and co-workers,[22] further speaking against consecutive two-photon processes. Despite an overall two-photon uptake, according to Figure 3, a linear rate growth suggests that a single-photon event is involved in the reaction rate-determining step.[23]

Synthetic Scope. Under the optimized conditions (Table 1, entry 1), we evaluated a variety of internal alkynes in the *peri*-(3 + 2) photocycloaddition reaction with methyl 8-quinoline carboxylate (**1a**) (Table 2A). Different aliphatic chains, ranging from ethyl (**3c**) to *n*-propyl (**3d**), *n*-butyl (**3a**), and *n*-pentyl (**3e**) could be installed at the bridging methylene, with excellent levels of *anti*-diastereoselectivity (>95:5 d.r.). Unsymmetrical disubstituted alkynes with similar steric demand at both ends delivered a separable mixture of regioisomers (**3f**, 46% combined yield).

Monosubstituted alkynes delivered the corresponding *peri*-bridged quinolines in moderate yields and excellent site selectivity (>95:5 r.r.) (Table 2B). In particular, the alkyne terminus was found to join C5, while the internal position connects to C4. This observation could be rationalized in terms of the initial attack onto the more sterically accessible and activated position to deliver substituted vinyl radicals.

Different alkyl substituents, from *n*-propyl (**3g**) to *n*-hexyl (**3h**), cyclohexyl (**3i**), and *iso*amyl (**3j**), were introduced at the C4-proximal bridge position. Methyl ether-containing product **3k** could also be obtained in a 31% yield. Benzoyl ester substitution was equally tolerated (**3l**). An array of quinoline-8-ketones—methyl, cyclohexyl, *iso*propyl, and cyclopentyl—reacted with terminal alkynes in modest yields (23−30%) and excellent regioselectivity to provide **3m**, **3n**, **3o**, and **3p**, respectively. Next, substitution at the heteroaromatic core was evaluated (Table 2C). 8-Quinoline esters featuring allyl (**3q**), trimethylsilyl (**3r**), methylcyclopropane (**3s**), and cyclohexyl (**3t**) groups delivered—when reacted with 5-decyne—the desired *peri*-(3 + 2) cycloaddition products in a 62−70% yield and with excellent anti-diastereoselectivity. In particular, the allyl group in **3q** offers a potential linchpin to incorporate *peri*-bridged quinoline motifs in more elaborated frameworks. Substituents proximal to the *peri*-4-position could be successfully accommodated (**3b**), as well as functional groups like highly fluorinated aliphatic chains (**3u**), aryl chloride (**3v**), and basic pyridine centers (**3w**). The reaction could tolerate free hydroxy and aliphatic chlorine groups without liability (**3x**), as well as sulfones (**3y**), which can serve as versatile synthetic intermediates.[24] A plethora of 8-quinoline ketones generated 4,5-*peri*-bridged quinolines: methyl (**3z**), *iso*propyl (**3aa**), cyclohexyl (**3ab**), and cyclopentyl (**3ac**) ketones were straightforwardly accommodated in 53−67% yield and with optimal diastereoselectivity (>95:5 d.r.). Phenethyl (**3ad**) and phenyl (**3ae**) ketone-substituted quinolines showed significantly attenuated reactivity, potentially due to unwanted π-stacking and change in energy-transfer properties, respectively. Substituted 6-fluoroquinoline delivered **3af** in 30% yield and excellent selectivity. Notably, phenanthroline—in which carbonyl EWGs are replaced by the condensed aza-arene—afforded C4-C5 *peri*-bridged product **3ag** with excellent *anti*-diastereoselectivity. Analogously, neocuproine could deliver product **3ah** in 39% yield. Given the fundamental importance of phenanthroline-based ligands in coordination chemistry,[25]

https://doi.org/10.1021/jacs.2c05687
J. Am. Chem. Soc. 2022, 144, 15662−15671

we can envisage the use of *peri*-bridged analogues as new ligands with unique steric properties.

Postsynthetic Modifications. The substituted *peri*-bridged quinoline core offers valuable synthetic linchpins toward further modification (Figure 4). Basic hydrolytic

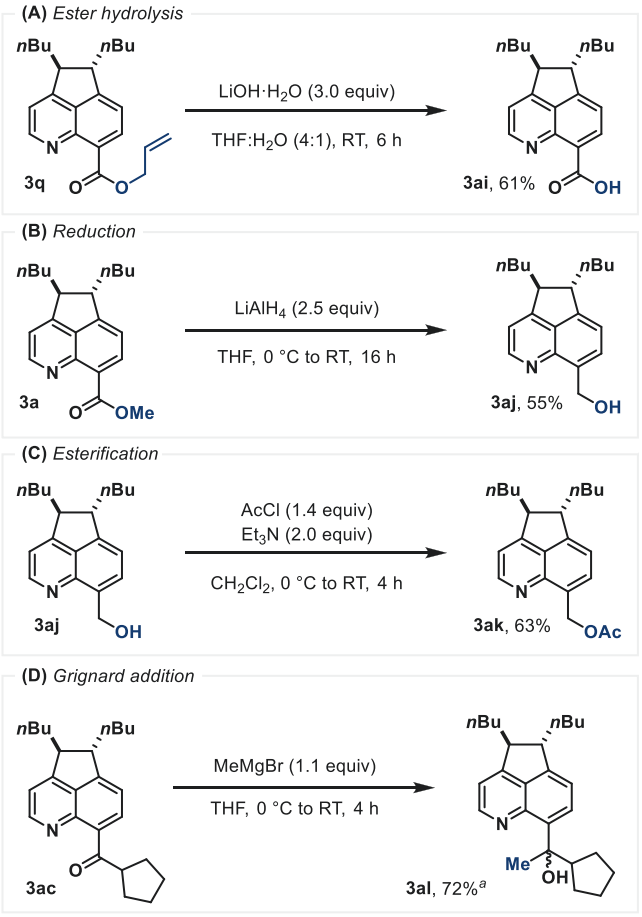

Figure 4. Postsynthetic modifications. (A) Basic ester hydrolysis. (B) Carbonyl reduction with lithium aluminum hydride. (C) Esterification. (D) Grignard addition. [a]Approx. 1:1 d.r., > 95:5 d.r. at the *peri*-bridge.

conditions afforded unprotected 8-quinoline carboxylic acid (**3ai**) from the corresponding allyl ester (**3q**). Ester **3a** could be smoothly converted to the corresponding benzylic alcohol **3aj** using lithium aluminum hydride in 55% yield. Furthermore, the free alcohol moiety allows for the conjugation of the tricyclic core via esterification, such as for product **3ak** from alcohol **3aj**. Ketone-bearing quinoline **3ac** underwent Grignard reagent addition to yield sterically encumbered tertiary alcohol **3al** in 72% yield.

CONCLUSIONS

In the realm of photocatalyzed cycloadditions of (hetero)-arenes, harnessing *peri*-(3 + 2) reaction modes represents a paradigm shift since established manifolds target a single ring of (hetero)aromatic systems. Overcoming typical monocyclic (4 + 2), (3 + 2), and (2 + 2) reaction manifolds, the presented strategy enables the one-step synthesis of challenging *peri*-bridged aza-acenaphthenes from simple quinolines and mono- and disubstituted alkynes. Adjoining seemingly remote carbon centers leverages a seldom explored energy-transfer/single-electron-transfer cascade[15] using a single photocatalytic system. Photosensitization of the quinoline moiety permits the *peri*-addition process to be both thermodynamically feasible and kinetically competitive (compressed kinetic barrier).[13] The ensuing SET events underlie an efficient rearomatization phase, which prevents both undesired cycloreversion and fosters traceless *peri*-C−H functionalization at the quinoline core. We anticipate that our findings will spur the further development of innovative aromatic cycloaddition technologies based on hybrid EnT/SET events, extending beyond (4 + 2) and (2 + 2) cycloadditions and targeting increasingly challenging molecular frameworks.

ASSOCIATED CONTENT

Supporting Information

The Supporting Information is available free of charge at https://pubs.acs.org/doi/10.1021/jacs.2c05687.

Experimental procedures, mechanistic studies, computational methods, energies, geometries of calculated structures, and analytical data (PDF)

AUTHOR INFORMATION

Corresponding Authors

K. N. Houk − *Department of Chemistry and Biochemistry, University of California, Los Angeles, California 90095-1569, United States;* orcid.org/0000-0002-8387-5261; Email: houk@chem.ucla.edu

Frank Glorius − *Westfälische Wilhelms-Universität Münster, Organisch-Chemisches Institut, 48149 Münster, Germany;* orcid.org/0000-0002-0648-956X; Email: glorius@uni-muenster.de

Authors

Peter Bellotti − *Westfälische Wilhelms-Universität Münster, Organisch-Chemisches Institut, 48149 Münster, Germany;* Present Address: Department of Pharmacology, Joan & Sanford I. Weill Medical College of Cornell University, New York 10021, New York, United States; orcid.org/0000-0001-9367-5100

Torben Rogge − *Department of Chemistry and Biochemistry, University of California, Los Angeles, California 90095-1569, United States;* orcid.org/0000-0002-4519-4596

Fritz Paulus − *Westfälische Wilhelms-Universität Münster, Organisch-Chemisches Institut, 48149 Münster, Germany*

Ranjini Laskar − *Westfälische Wilhelms-Universität Münster, Organisch-Chemisches Institut, 48149 Münster, Germany*

Nils Rendel − *Westfälische Wilhelms-Universität Münster, Organisch-Chemisches Institut, 48149 Münster, Germany*

Jiajia Ma − *Westfälische Wilhelms-Universität Münster, Organisch-Chemisches Institut, 48149 Münster, Germany;* Present Address: Frontiers Science Center for Transformative Molecules, School of Chemistry and Chemical Engineering, Shanghai Jiao Tong University, Shanghai 200240, P. R. China.

Complete contact information is available at: https://pubs.acs.org/10.1021/jacs.2c05687

Author Contributions

[⊥]P.B., T.R., and F.P. contributed equally to this work.

Funding

This work was generously supported by the Deutsche Forschungsgemeinschaft (Leibniz Award, F.G.; SBF 858,

P.B.; IRTG 2678, F.P.), the Deutscher Akademischer Austauschdienst (R.L.), the National Science Foundation (CHE-1764328 to K.N.H.), and the Alexander von Humboldt-Foundation (Feodor Lynen fellowship, T.R.).

Notes

The authors declare no competing financial interest.

Raw NMR data (JCAMP-DX files) for literature unknown compounds and mechanistic experiments, raw Stern−Volmer quenching analysis data, and Cartesian coordinates of optimized structures have been deposited at Zenodo under the Creative Commons Attribution 4.0 International license. DOI: 10.5281/zenodo.6954263.

■ ACKNOWLEDGMENTS

The authors thank Prof. Manuel van Gemmeren (Christian-Albrechts-Universität zu Kiel) and Mirxan Farizyan (WWU Münster) for the generous donation of HFIP-d_1, Dr. Jian-Heng Ye (WWU Münster) for providing alkyne **2k**, and Dr. Tiffany Paulisch (WWU Münster) for providing a sample of *fac*-[Ir(CF_3-pmb)$_3$]. The NMR laboratory of the Organic Chemistry Institute (WWU Münster) is acknowledged for experimental assistance with the NMR measurements. Calculations were performed on the Hoffman2 cluster at the University of California, Los Angeles.

■ REFERENCES

(1) Nicolaou, K. C.; Snyder, S. A.; Montagnon, T.; Vassilikogiannakis, G. The Diels−Alder Reaction in Total Synthesis. *Angew. Chem. Int. Ed.* **2002**, *41*, 1668−1698.

(2) For total synthesis approaches towards delavatine A: (a) Zhang, Z.; Wang, J.; Li, J.; Yang, F.; Liu, G.; Tang, W.; He, W.; Fu, J.-J.; Shen, Y.-H.; Li, A.; Zhang, W.-D. Total Synthesis and Stereochemical Assignment of Delavatine A: Rh-Catalyzed Asymmetric Hydrogenation of Indene-Type Tetrasubstituted Olefins and Kinetic Resolution through Pd-Catalyzed Triflamide-Directed C−H Olefination. *J. Am. Chem. Soc.* **2017**, *139*, 5558−5567. (b) Peez, T.; Luy, J.-N.; Harms, K.; Tonner, R.; Koert, U. From Acenaphthenes to (+)-Delavatine A: Visible-Light-Induced Ring Closure of Methyl (α-Naphthyl) Acrylates. *Chem. Eur. J.* **2018**, *24*, 17686−17690. (c) Palani, V.; Hugelshofer, C. L.; Kevlishvili, I.; Liu, P.; Sarpong, R. A Short Synthesis of Delavatine A Unveils New Insights into Site-Selective Cross-Coupling of 3,5-Dibromo-2-pyrone. *J. Am. Chem. Soc.* **2019**, *141*, 2652−2660. (d) Palani, V.; Hugelshofer, C. L.; Sarpong, R. A Unified Strategy for the Enantiospecific Total Synthesis of Delavatine A and Formal Synthesis of Incarviatone A. *J. Am. Chem. Soc.* **2019**, *141*, 14421−14432.

(3) Sugimori, M.; Ejima, A.; Ohsuki, S.; Uoto, K.; Mitsui, I.; Matsumoto, K.; Kawato, Y.; Yasuoka, M.; Sato, K. Antitumor Agents. VII. Synthesis and Antitumor Activity of Novel Hexacyclic Camptothecin Analogs. *J. Med. Chem.* **1994**, *37*, 3033−3039.

(4) (a) Tsantrizos, Y. S.; Bailey, M. D.; Bilodeau, F.; Carson, R. J.; Coulombe, R.; Fader, L.; Halmos, T.; Kawai, S.; Landry, S.; Laplante, S.; Morin, S.; Parisien, M.; Poupart, M.-A.; Simoneau, B. Inhibitors of Human Immunodeficiency Virus Replication. Patent WO2009062285, May 22, 2009. (b) Li, W.; De Croos, P.; Fandrick, K. R.; Gao, J. J.; Haddad, N.; Lu, Z.-H.; Qu, B.; Rodriguez, S.; Senanayake, C. H.; Zhang, Y.; Tang, W. Process for the Preparation of an HIV Integrase Inhibitor. Patent WO2012138670, October 11, 2012.

(5) Schmidt, R.; Griesbaum, K.; Behr, A.; Biedenkapp, D.; Voges, H.-W.; Garbe, D.; Paetz, C.; Collin, G.; Mayer, D.; Höke H. Hydrocarbons. In *Ullmann's Encyclopedia of Industrial Chemistry*; Wiley-VCH, 2015.

(6) Selected strategies featuring methylene bridge formation in (aza) acenaphthenes from dangling alkenes (a) Lapouyade, R.; Koussini, R.; Rayez, J.-C. Photocyclisation of 1,1-diarylethylenes; the novel formation of a five-membered ring. *J. Chem. Soc., Chem. Commun.* **1975**, 676−677. (b) Lapouyade, R.; Koussini, R.; Bouas-Laurent, H. Primary and tertiary amines as catalysts of hydrogen transfer in the photocyclization of 1,1-diarylethylenes. *J. Am. Chem. Soc.* **1977**, *99*, 7374−7376. (c) Clayton, M. D.; Marcinow, Z.; Rabideau, P. W. Benzeneseleninic anhydride oxidation of 1,2-diarylethanes and 1,2-diarylethylenes to 1,2-diaryldiketones. *Tetrahedron Lett.* **1998**, *39*, 9127−9130. (d) Ansems, R. B. M.; Scott, L. T. Circumtrindene: A Geodesic Dome of Molecular Dimensions. Rational Synthesis of 60 of C_{60}[1]. *J. Am. Chem. Soc.* **2000**, *122*, 2719−2724. (e) Lahore, S.; Narkhede, U.; Merlini, L.; Dallavalle, S. Total Synthesis of the Natural Product Benzo[*j*]fluoranthene-4,9-diol: An Approach to the Synthesis of Oxygenated Benzo[*j*]fluoranthenes. *J. Org. Chem.* **2013**, *78*, 10860−10866.

(7) Repke, D. B.; Jahangir; Clark, R. D.; Nelson, J. T.; MacLean, D. B. Synthesis of naucléfine, angustidine, angustine, (±)-13b,14-dihydro-angustine and naulafine. *Tetrahedron* **1989**, *45*, 2541−2550.

(8) Selected strategies featuring aromatic ring closure towards (aza) acenaphthenes (a) Fourmigué, M.; Boubekeur, K.; Batail, P.; Bechgaard, K. Azonia Derivatives of Arenes: Synthesis and Properties of 10c-Azoniafluoranthene. *Angew. Chem. Int. Ed.* **1989**, *28*, 588−590. (b) Zhang, G.; Rominger, F.; Mastalerz, M. Fused π-Extended Truxenes via a Threefold Borylation as the Key Step. *Chem. Eur. J.* **2016**, *22*, 3084−3093.

(9) For selected reviews on energy-transfer photocatalysis: (a) Strieth-Kalthoff, F.; James, M. J.; Teders, M.; Pitzer, L.; Glorius, F. Energy transfer catalysis mediated by visible light: principles, applications, directions. *Chem. Soc. Rev.* **2018**, *47*, 7190−7202. (b) Zhou, Q.-Q.; Zou, Y.-Q.; Lu, L.-Q.; Xiao, W.-J. Visible-Light-Induced Organic Photochemical Reactions through Energy-Transfer Pathways. *Angew. Chem.Int. Ed.* **2019**, *58*, 1586−1604. (c) Strieth-Kalthoff, F.; Glorius, F. Triplet Energy Transfer Photocatalysis: Unlocking the Next Level. *Chem* **2020**, *6*, 1888−1903.

(10) For selected reviews dealing with energy-transfer dearomative cycloaddition reactions: (a) Cheng, Y.-Z.; Feng, Z.; Zhang, X.; You, S.-L. Visible-light induced dearomatization reactions. *Chem. Soc. Rev.* **2022**, *51*, 2145−2170. (b) Oderinde, M. S.; Jin, S.; Dhar, T. J. M.; Meanwell, N. A.; Mathur, A.; Kempson, J. Advances in the synthesis of three-dimensional molecular architectures by dearomatizing photocycloadditions. *Tetrahedron* **2022**, *103*, No. 132087.

(11) For selected (2 + 2)-dearomative cycloaddition strategies: (a) Zhu, M.; Zheng, C.; Zhang, X.; You, S.-L. Synthesis of Cyclobutane-Fused Angular Tetracyclic Spiroindolines via Visible-Light-Promoted Intramolecular Dearomatization of Indole Derivatives. *J. Am. Chem. Soc.* **2019**, *141*, 2636−2644. (b) Zhu, M.; Zhang, X.; Zheng, C.; You, S.-L. Visible-Light-Induced Dearomatization via [2+2] Cycloaddition or 1,5-Hydrogen Atom Transfer: Divergent Reaction Pathways of Transient Diradicals. *ACS Catal.* **2020**, *10*, 12618−12626. (c) Zhu, M.; Xu, H.; Zhang, X.; Zheng, C.; You, S.-L. Visible-Light-Induced Intramolecular Double Dearomative Cycloaddition of Arenes. *Angew. Chem. Int. Ed.* **2021**, *60*, 7036−7040. (d) Oderinde, M. S.; Ramirez, A.; Dhar, T. G. M.; Cornelius, L. A. M.; Jorge, C.; Aulakh, D.; Sandhu, B.; Pawluczyk, J.; Sarjeant, A. A.; Meanwell, N. A.; Mathur, A.; Kempson, J. Photocatalytic Dearomative Intermolecular [2 + 2] Cycloaddition of Heterocycles for Building Molecular Complexity. *J. Org. Chem.* **2021**, *86*, 1730−1747. (e) Oderinde, M. S.; Mao, E.; Ramirez, A.; Pawluczyk, J.; Jorge, C.; Cornelius, L. A. M.; Kempson, J.; Vetrichelvan, M.; Pitchai, M.; Gupta, A.; Gupta, A. K.; Meanwell, N. A.; Mathur, A.; Murali Dhar, T. G. Synthesis of Cyclobutane-Fused Tetracyclic Scaffolds via Visible-Light Photocatalysis for Building Molecular Complexity. *J. Am. Chem. Soc.* **2020**, *142*, 3094−3103. (f) Rolka, A. B.; König, B. Dearomative Cycloadditions Utilizing an Organic Photosensitizer: An Alternative to Iridium Catalysis. *Org. Lett.* **2020**, *22*, 5035−5040. (g) James, M. J.; Schwarz, J. L.; Strieth-Kalthoff, F.; Wibbeling, B.; Glorius, F. Dearomative Cascade Photocatalysis: Divergent Synthesis through Catalyst Selective Energy Transfer. *J. Am. Chem. Soc.* **2018**, *140*, 8624−8628. (h) Strieth-Kalthoff, F.; Henkel, C.; Teders, M.; Kahnt, A.; Knolle, W.; Gómez-Suárez, A.; Dirian, K.; Alex, W.; Bergander, K.;

Daniliuc, C. G.; Abel, B.; Guldi, D. M.; Glorius, F. Discovery of Unforeseen Energy-Transfer-Based Transformations Using a Combined Screening Approach. *Chem* **2019**, *5*, 2183−2194. (i) Zhang, Z.; Yi, D.; Zhang, M.; Wei, J.; Lu, J.; Yang, L.; Wang, J.; Hao, N.; Pan, X.; Zhang, S.; Wie, S.; Fu, Q. Photocatalytic Intramolecular [2 + 2] Cycloaddition of Indole Derivatives via Energy Transfer: A Method for Late-Stage Skeletal Transformation. *ACS Catal.* **2020**, *10*, 10149−10156.

(12) For (4 + 2)-dearomative cycloaddition strategies: (a) Ma, J.; Strieth-Kalthoff, F.; Dalton, T.; Freitag, M.; Schwarz, J. L.; Bergander, K.; Daniliuc, C.; Glorius, F. Direct Dearomatization of Pyridines via an Energy-Transfer-Catalyzed Intramolecular [4+2] Cycloaddition. *Chem* **2019**, *5*, 2854−2864. (b) Ma, J.; Chen, S.; Bellotti, P.; Guo, R.; Schäfer, F.; Heusler, A.; Zhang, X.; Daniliuc, C.; Brown, M. K.; Houk, K. N.; Glorius, F. Photochemical intermolecular dearomative cycloaddition of bicyclic azaarenes with alkenes. *Science* **2021**, *371*, 1338−1345. (c) Morofuji, T.; Nagai, S.; Chitose, Y.; Abe, M.; Kano, N. Protonation-Enhanced Reactivity of Triplet State in Dearomative Photocycloaddition of Quinolines to Olefins. *Org. Lett.* **2021**, *23*, 6257−6261. (d) Ma, J.; Chen, S.; Bellotti, P.; Wagener, T.; Daniliuc, C.; Houk, K. N.; Glorius, F. Facile access to fused 2D/3D rings via intermolecular cascade dearomative [2+2] cycloaddition/rearrangement reactions of quinolines with alkenes. *Nat. Catal.* **2022**, *5*, 405−413.

(13) Remy, R.; Bochet, C. G. Arene−Alkene Cycloaddition. *Chem. Rev.* **2016**, *116*, 9816−9849.

(14) (a) Tietze, L. F.; Beifuss, U. Sequential Transformations in Organic Chemistry: A Synthetic Strategy with a Future. *Angew. Chem., Int. Ed.* **1993**, *32*, 131−163. (b) Tietze, L. F. Domino Reactions in Organic Synthesis. *Chem. Rev.* **1996**, *96*, 115−136. (c) Tietze, L. F. *Domino Reactions: Concepts for Efficient Organic Synthesis*; Wiley-WCH, 2014.

(15) Selected examples of dual EnT/SET tactics (a) Xuan, J.; Xia, X.-D.; Zeng, T.-T.; Feng, Z.-J.; Chen, J.-R.; Lu, L.-Q.; Xiao, W.-J. Visible-Light-Induced Formal [3+2] Cycloaddition for Pyrrole Synthesis under Metal-Free Conditions. *Angew. Chem. Int. Ed.* **2014**, *53*, 5653−5656. (b) Metternich, J. B.; Gilmour, R. One Photocatalyst, *n* Activation Modes Strategy for Cascade Catalysis: Emulating Coumarin Biosynthesis with (−)-Riboflavin. *J. Am. Chem. Soc.* **2016**, *138*, 1040−1045. (c) Tiwari, D. K.; Maurya, R. A.; Nanubolu, J. B. Visible-Light/Photoredox-Mediated sp^3 C−H Functionalization and Coupling of Secondary Amines with Vinyl Azides in Flow Microreactors. *Chem. Eur. J.* **2016**, *22*, 526−530. (d) Chandrasekhar, D.; Borra, S.; Nanubolu, J. B.; Maurya, R. A. Visible Light Driven Photocascade Catalysis: $Ru(bpy)_3(PF_6)_2$/TBHP-Mediated Synthesis of Fused β-Carbolines in Batch and Flow Microreactors. *Org. Lett.* **2016**, *18*, 2974−2977. (e) Borra, S.; Chandrasekhar, D.; Adhikary, S.; Rasala, S.; Gokulnath, S.; Maurya, R. A. Visible-Light Driven Photocascade Catalysis: Union of *N*,*N*-Dimethylanilines and α-Azidochalcones in Flow Microreactors. *J. Org. Chem.* **2017**, *82*, 2249−2256. (f) Hossain, A.; Pagire, S. K.; Reiser, O. Visible-Light-Mediated Synthesis of Pyrazines from Vinyl Azides Utilizing a Photocascade Process. *Synlett* **2017**, *28*, 1707−1714. (g) Lin, Q.-Y.; Xu, X.-H.; Qing, F.-L. Chemo-, Regio-, and Stereoselective Trifluoromethylation of Styrenes via Visible Light-Driven Single-Electron Transfer (SET) and Triplet−Triplet Energy Transfer (TTET) Processes. *J. Org. Chem.* **2014**, *79*, 10434−10446. (h) Bao, L.; Cheng, J.-T.; Wang, Z.-X.; Chen, X.-Y. Pyrylium salts acting as both energy transfer and electron transfer photocatalysts for $E \rightarrow Z$ isomerization of activated alkenes and cyclization of cinnamic or biaryl carboxylic acids. *Org. Chem. Front.* **2022**, *9*, 973−978.

(16) For selected reports: (a) Lee, S.; Chataigner, I.; Piettre, S. R. Facile Dearomatization of Nitrobenzene Derivatives and Other Nitroarenes with *N*-Benzyl Azomethine Ylide. *Angew. Chem. Int. Ed.* **2011**, *50*, 472−476. (b) Trost, B. M.; Ehmke, V.; O'Keefe, M.; Bringley, D. A. Palladium-Catalyzed Dearomative Trimethylenemethane Cycloaddition Reactions. *J. Am. Chem. Soc.* **2014**, *136*, 8213−8216. (c) Awata, A.; Arai, T. PyBidine/Copper Catalyst: Asymmetric *exo*′-Selective [3+2] Cycloaddition using Imino Ester and Electrophilic Indole. *Angew. Chem. Int. Ed.* **2014**, *53*, 10462−10465. (d) Wang, H.; Zhang, J.; Tu, H.; Zhang, J. Phosphine-Catalyzed Enantioselective Dearomative [3+2]-Cycloaddition of 3-Nitroindoles and 2-Nitrobenzofurans. *Angew. Chem. Int. Ed.* **2019**, *58*, 5422−5426. (e) Li, K.; Gonçalves, T. P.; Huang, K.-W.; Lu, Y. Dearomatization of 3-Nitroindoles by a Phosphine-Catalyzed Enantioselective [3+2] Annulation Reaction. *Angew. Chem. Int. Ed.* **2019**, *58*, 5427−5431.

(17) (a) Ballinger, P.; Long, F. A. Acid Ionization Constants of Alcohols. II. Acidities of Some Substituted Methanols and Related Compounds. *J. Am. Chem. Soc.* **1960**, *82*, 795−798. (b) Colomer, I.; Chamberlain, A. E. R.; Haughey, M. B.; Donohoe, T. J. Hexafluoroisopropanol as a highly versatile solvent. *Nat. Rev. Chem.* **2017**, *1*, No. 0088. (c) Motiwala, H. F.; Armaly, A. M.; Cacioppo, J. C.; Coombs, T. C.; Koehn, K. R. K.; Norwood, V. M. I. V.; Aubé, J. HFIP in Organic Synthesis. *Chem. Rev.* **2022**, *122*, 12544−12747. (d) Dyatkin, B. L.; Mochalina, E. P.; Knunyants, I. L. The acidic properties of fluorine-containing alcohols, hydroxylamines and oximes. *Tetrahedron* **1965**, *21*, 2991−2995.

(18) (a) Paulisch, T. O.; Mai, L. A.; Strieth-Kalthoff, F.; James, M. J.; Henkel, C.; Guldi, D. M.; Glorius, F. Dynamic Kinetic Sensitization of β-Dicarbonyl Compounds—Access to Medium-Sized Rings by De Mayo-Type Ring Expansion. *Angew. Chem. Int. Ed.* **2022**, *61*, No. e202112695. (b) Tamayo, A. B.; Alleyne, B. D.; Djurovich, P. I.; Lamansky, S.; Tsyba, I.; Ho, N. N.; Bau, R.; Thompson, M. E. Synthesis and Characterization of Facial and Meridional Tris-cyclometalated Iridium(III) Complexes. *J. Am. Chem. Soc.* **2003**, *125*, 7377−7387. (c) Romero, N. A.; Nicewicz, D. A. Organic Photoredox Catalysis. *Chem. Rev.* **2016**, *116*, 10075−10166. (d) Slinker, J. D.; Gorodetsky, A. A.; lowry, M. S.; Wang, J.; Parker, S.; Rohl, R.; Bernhard, S.; Malliaras, G. G. Efficient Yellow Electroluminescence from a Single Layer of a Cyclometalated Iridium Complex. *J. Am. Chem. Soc.* **2004**, *126*, 2763−2767. (e) Lowry, M. S.; Goldsmith, J. I.; Slinker, J. D.; Rohl, R.; Pascal, R. A.; Malliaras, G. G.; Bernhard, S. Single-Layer Electroluminescent Devices and Photoinduced Hydrogen Production from an Ionic Iridium(III) Complex. *Chem. Mater.* **2005**, *17*, 5712−5719. (f) Kalyanasundaram, K. Photophysics, photochemistry and solar energy conversion with tris(bipyridyl)ruthenium(II) and its analogues. *Coord. Chem. Rev.* **1982**, *46*, 159−244. (g) Pitzer, L.; Sandfort, F.; Strieth-Kalthoff, F.; Glorius, F. Carbonyl-Olefin Cross-Metathesis Through a Visible-Light-Induced 1,3-Diol Formation and Fragmentation Sequence. *Angew. Chem. Int. Ed.* **2018**, *57*, 16219−16223.

(19) Pitzer, L.; Schäfers, F.; Glorius, F. Rapid Assessment of the Reaction-Condition-Based Sensitivity of Chemical Transformations. *Angew. Chem. Int. Ed.* **2019**, *58*, 8572−8576.

(20) Selected examples showing E_T correlation: (a) Patra, T.; Bellotti, P.; Strieth-Kalthoff, F.; Glorius, F. Photosensitized Intermolecular Carboimination of Alkenes through the Persistent Radical Effect. *Angew. Chem. Int. Ed.* **2020**, *59*, 3172−3177. (b) Patra, T.; Das, M.; Daniliuc, C. G.; Glorius, F. Metal-free photosensitized oxyimination of unactivated alkenes with bifunctional oxime carbonates. *Nat. Catal.* **2021**, *4*, 54−61. (c) Becker, M. R.; Wearing, E. R.; Schindler, C. S. Synthesis of azetidines via visible-light-mediated intermolecular [2+2] photocycloadditions. *Nat. Chem.* **2020**, *12*, 898−905. (d) Kleinmans, R.; Pinkert, T.; Dutta, S.; Paulisch, T. O.; Keum, H.; Daniliuc, C. G.; Glorius, F. Intermolecular [2π+2σ]-photocycloaddition enabled by triplet energy transfer. *Nature* **2022**, *605*, 477−482.

(21) (a) Chai, J.-D.; Head-Gordon, M. Long-range corrected hybrid density functionals with damped atom−atom dispersion corrections. *Phys. Chem. Chem. Phys.* **2008**, *10*, 6615−6620. (b) Weigend, F.; Ahlrichs, R. Balanced basis sets of split valence, triple zeta valence and quadruple zeta valence quality for H to Rn: Design and assessment of accuracy. *Phys. Chem. Chem. Phys.* **2005**, *7*, 3297−3305. (c) Marenich, A. V.; Cramer, C. J.; Truhlar, D. G. Universal Solvation Model Based on Solute Electron Density and on a Continuum Model of the Solvent Defined by the Bulk Dielectric Constant and Atomic Surface Tensions. *J. Phys. Chem. B* **2009**, *113*, 6378−6396.

https://doi.org/10.1021/jacs.2c05687
J. Am. Chem. Soc. 2022, 144, 15662−15671

(22) Chatterjee, A.; König, B. Birch-Type Photoreduction of Arenes and Heteroarenes by Sensitized Electron Transfer. *Angew. Chem. Int. Ed.* **2019**, *58*, 14289−14294.
(23) Glaser, F.; Kerzig, C.; Wenger, O. S. Multi-Photon Excitation in Photoredox Catalysis: Concepts, Applications, Methods. *Angew. Chem. Int. Ed.* **2020**, *59*, 10266−10284.
(24) Trost, M. B.; Kalnmals, C. A. Sulfones as Chemical Chameleons: Versatile Synthetic Equivalents of Small-Molecule Synthons. *Chem. Eur. J.* **2019**, *25*, 11193−11213.
(25) Bencini, A.; Lippolis, V. 1,10-Phenanthroline: A versatile building block for the construction of ligands for various purposes. *Coord. Chem. Rev.* **2010**, *254*, 2096−2180.

https://doi.org/10.1021/jacs.2c05687
J. Am. Chem. Soc. 2022, 144, 15662−15671